Zeitschrift: IABSE reports = Rapports AIPC = IVBH Berichte
Band: 79 (1998)

Artikel: Applicability of Dischinger-type to ultra-long span bridges
Autor: Narita, Nobuyuki / Nakamura, Hitoshi / Maeda, Ken-ichi
DOI: https://doi.org/10.5169/seals-59844

Applicability of Dischinger-Type to Ultra-Long Span Bridges

Nobuyuki NARITA
Prof.
Tokyo Metropolitan Univ.
Hachiouji, Japan

Hitoshi NAKAMURA
Res. Associate
Tokyo Metropolitan Univ.
Hachiouji, Japan

Ken-ichi MAEDA
Prof.
Tokyo Metropolitan Univ.
Hachiouji, Japan

Kunikatsu NOMURA
Res. Eng.
Kawada Industries Inc.
Tokyo, Japan

Summary

In this study, trial designs of Dischinger-type cable-stayed suspension bridges with a center span of 2,500 m, in which ratios of suspended parts were used as variable, were performed. Three types of cable-stayed suspension bridge models and the suspension bridge model were constructed. On comparing the weight of steel of superstructures from the results of trial designs, cable-stayed suspension bridges were superior to the suspension bridge considering the scale of substructures. In addition, buckling stability analyses and coupled flutter analyses for all types were carried out. From the results, it was found that cable-stayed suspension bridges were stable enough in buckling problems, and had the critical wind velocity higher than the suspension bridge. Therefore, the authors confirmed that Dischinger-type cable-stayed suspension bridges were competitive with suspension bridges as ultra-long span bridges.

1. Introduction

Realization of ultra-long span bridges with a span length ranging from 2,000 m to 3,000 m is influenced by their aerodynamic stability. Accordingly, for the construction of next- generation bridges following the Akashi-Kaikyo Bridge, research on new cable-supported bridges with high economic efficiency and high torsional rigidity is attracting much attention. We have already proposed a Dischinger-type cable-stayed suspension bridge as a long-span bridge, which replaces a cable-stayed bridge whose maximum possible span length is assumed to be 1,500 m [1], and predicted that it is feasible to apply for ultra-long span bridges [2]. The torsional rigidity in the cable-stayed suspension bridge is increased due to a combination of a streamlined stiffening box-girder suspension bridge and a cable-stayed bridge. In this study, we executed a trial design of this bridge by setting the center span length at 2,500 m and varying the length of the suspended parts. In addition, focusing on the buckling and aerodynamic stabilities of the bridges, we investigated its applicability and feasibility as an ultra-long span bridge.

2. Design concept and trial design

2.1 Analysis model and trial design

Using models with a center span length of 2,500 m for a rough investigation, we executed trial designs of three types of cable-stayed suspension bridges with different ratios of suspended part length to stayed part length, as well as a suspension bridge, as shown in *Figure 1*, with the aim of highlighting their structural characteristics with varying suspended part length. The suspended part lengths of the center span were 960, 1,280 and 1,600 m in Type-1, Type-2 and Type-3 models, respectively. The suspension bridge model is the Type-4 model. The height of the main tower was varied in accordance with stayed part lengths. *Table 1* shows cross-

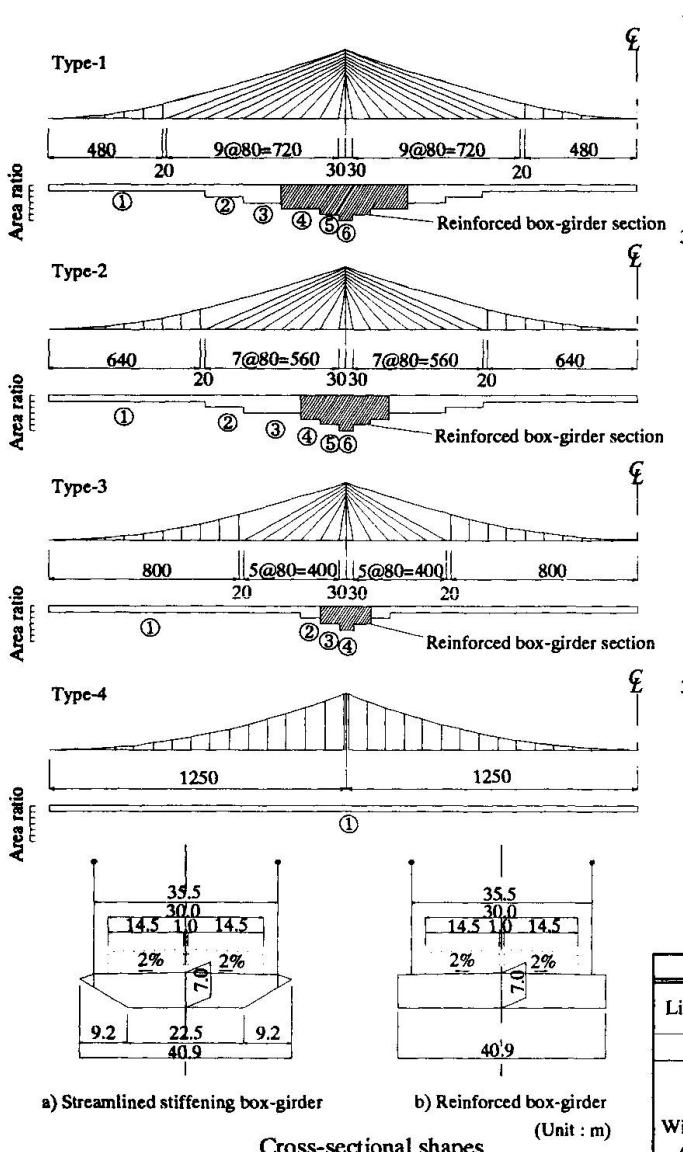

Cross-sectional shapes

Fig. 1 Analysis models

Table 1 Cross-sectional properties

Type-1

	①	②	③	④	⑤	⑥
$A_G(m^2)$	1.614	2.191	2.828	3.141	3.418	3.695
$I_{G,in}(m^4)$	13.304	18.304	23.667	30.061	31.088	32.11
$I_{G,out}(m^4)$	230.576	322.523	410.358	573.465	689.233	805.001
$J_G(m^4)$	26.923	37.284	51.388	70.565	73.161	74.365
$A_{mc}(m^2)$	side span : 0.418			center span : 0.405		
$A_{ac}(m^2)$	0.01861~0.05585					

Type-2

	①	②	③	④	⑤	⑥
$A_G(m^2)$	1.614	1.645	2.191	2.408	2.553	2.685
$I_{G,in}(m^4)$	13.304	13.366	18.304	23.656	24.181	24.659
$I_{G,out}(m^4)$	230.576	240.353	322.523	438.702	499.342	554.469
$J_G(m^4)$	26.923	27.172	37.284	50.843	52.571	53.415
$A_{mc}(m^2)$	side span : 0.584			center span : 0.575		
$A_{ac}(m^2)$	0.01577~0.04851					

Type-3

	①	②	③	④
$A_G(m^2)$	1.614	1.733	1.992	2.058
$I_{G,in}(m^4)$	13.304	14.307	18.943	19.182
$I_{G,out}(m^4)$	230.576	253.457	381.682	409.246
$J_G(m^4)$	26.923	29.932	41.663	42.296
$A_{mc}(m^2)$	side span : 0.739		center span : 0.731	
$A_{ac}(m^2)$	0.01366~0.03861			

Type-4

	①
$A_G(m^2)$	1.614
$I_{G,in}(m^4)$	13.304
$I_{G,out}(m^4)$	230.576
$J_G(m^4)$	26.923
$A_{mc}(m^2)$	0.870

Main tower

	/column
$A_T(m^2)$	3.000~5.796
$I_{T,in}(m^4)$	22.6~45.9
$I_{T,out}(m^4)$	42.3~131.0
$J_T(m^4)$	33.0~46.0

Table 2 Load conditions

		Type-1	Type-2	Type-3	Type-4
Live load	Concentrated(tf)	167.365			
	Distributed(tf/m)	3.906			
Temperature(℃)		±30			
Wind load (tf/m)	Girder	3.233			
	Tower	19.133	18.733	18.451	18.451
	Main Cable	0.658	0.777	0.876	1.043
	Stay Cable	0.133 ~0.206	0.124 ~0.185	0.163 ~0.116	——

sectional properties in each model. In all models, the cross-sectional depth of the main girder was 7 m. A static calculation was performed on the basis of the basic cross section of 12-mm upper flange thickness and 10-mm lower flange thickness. The cross sections that exceeded allowable stress were treated by an increase in the plate thickness. In the calculations, design and load conditions were in accordance with design specifications of Honshu-Shikoku Authority [3]. For the cable-stayed suspension bridges, a linearized finite displacement analysis was applied for the influence line in-plane analysis, and a finite displacement analysis was applied for the out-of-plane wind load analysis. For the suspension bridge, a deflection theory analysis expressed as stiffness matrix formula and Moisseiff's lateral load analysis were applied for the respective analyses.

Figure 2 shows member-end forces and deformations of the above four models, when dead loads, live loads and thermal forces were applied, and when wind loads with a design basic wind speed U_{10} of 50 m/s was applied. *Table 2* shows load conditions in these analyses.

Results of the trial design showed that the member-end force generated at the main girder of the suspension bridge was a fairly small; the maximum stress generated on the basic cross section due to in-plane bending moment and out-of-plane bending moment was 400 kgf/cm^2 and 1,300 kgf/cm^2, respectively.

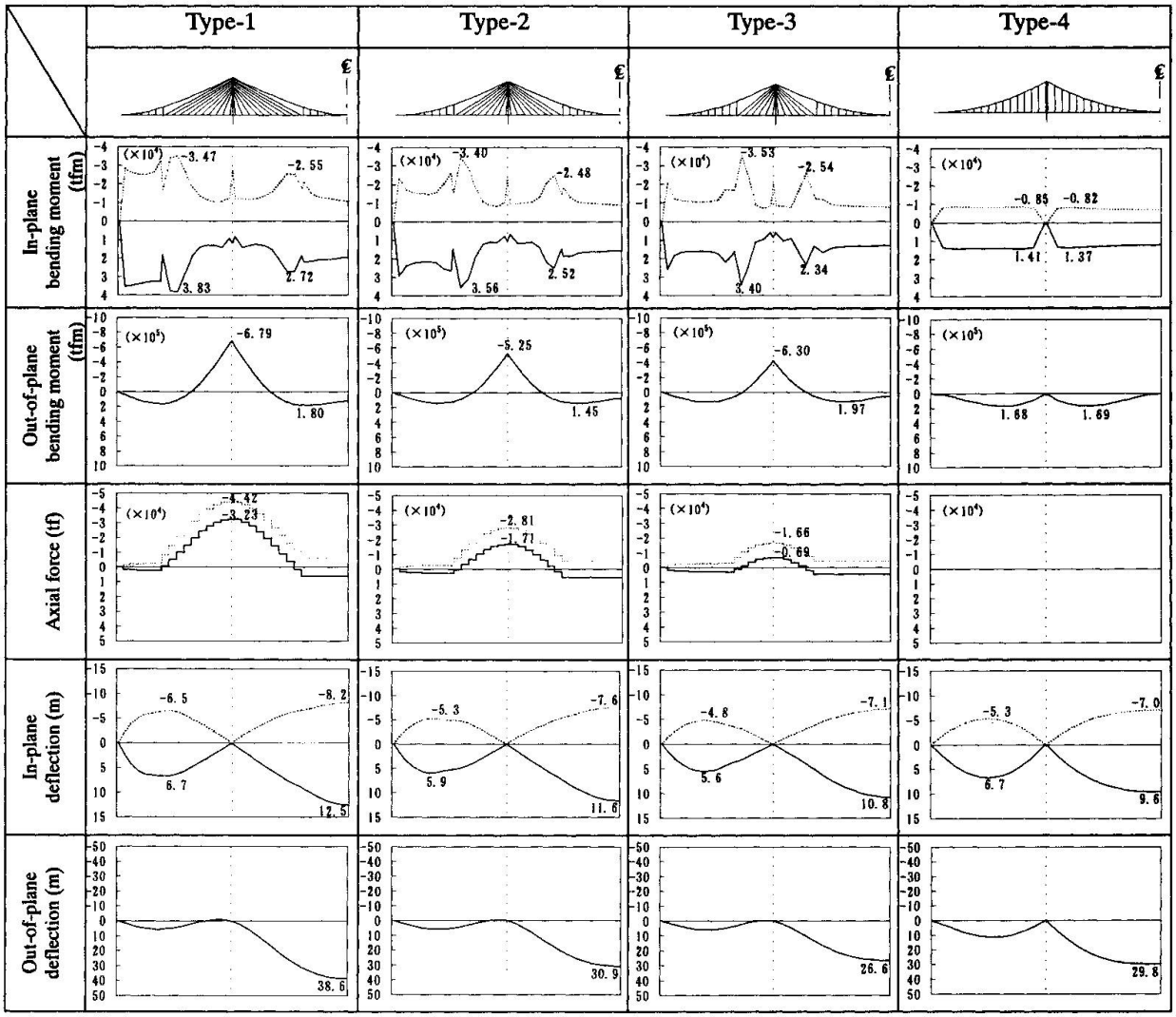

Fig. 2 Member-end forces and deformations of main girders

In the cable-stayed suspension bridges, basic cross sections of the suspended part did not exhibit any problems in terms of stress. However, at the stayed parts, since the out-of-plane bending moment due to axial force and wind load increases, it was necessary to use the reinforced box-girder as shown in *Figure 1 b)*, in addition to increasing the plate thickness near the main tower of the main girder.

In-plane deflection in the cable-stayed suspension bridges was larger than that in the suspension bridge. The deflection tended to increase with increasing suspended part length. With respect to out-of-plane deflection, the amount of deformation was the largest in Type-1, and the smallest in Type-3. The amounts of out-of-plane deflection in Type-2 and Type-4 were similar.

2.2 Comparison of weight of steel

Figure 3 shows the results of the calculation of steel weight. The ratio of weight of main girder and main tower to total steel weight was the largest for Type-1 among the 4 models, and the total steel weight for Type-1 was the largest, weighing approximately 250,000 tf. In contrast, although the weight of the main girder and main tower of the Type-2 cable-stayed suspension bridge is higher than that of Type-4, total steel weight of Type-2 was almost the same as that of Type-4 since the weight of the cable is lower in Type-2; the total steel weight of Type-2 was approximately 230,000tf. The calculated results showed that the total steel weight of Type-3 was the lowest. In the Type-4 suspension bridge, the weight of the main cable, which involves a fairly high cost of construction, was the highest. Accordingly, the economic efficiency of the Type-4 suspension bridge is lower than that of Type-2 when the cost of the

superstructure is taken into account. Considering the total cost including those of the superstructure and the substructure, the difference in the construction cost between the two types of bridges is predicted to increase. Thus, cable-stayed suspension bridges can be sufficiently competitive with suspension bridges in terms of economic efficiency, when an appropriate suspended part length is set, as observed in the case of Type-2.

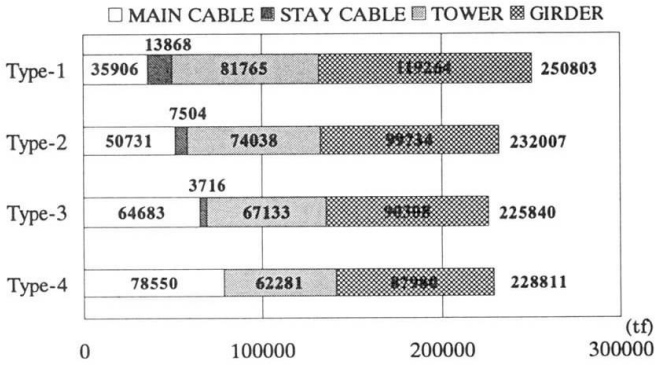

Fig. 3 Comparison of weight of steel

3. Stability check

In cable-stayed suspension bridges, axial force of the main girder becomes dominant with an increase in the stayed part length, which leads to a problem in buckling stability. Therefore, we conducted a stability check related to the main girder cross section, at the position of the main tower where the main girder axial force is maximum, using the following equation of stability check based on the specifications for highway bridges [4].

$$\frac{\sigma_c}{\sigma_{ca}} + \frac{\sigma_{bc}}{\sigma_{bao}\left(1-\sigma_c/\sigma_{ea}\right)} \le 1 \quad , \quad \sigma_{ca} = \sigma_{cag} \cdot \sigma_{cal} / \sigma_{cao} \quad , \quad \ell_e = \pi\sqrt{\frac{EI}{\lambda N}}$$

where :
- σ_c : Compressive stress due to axial force acting on the sections were stress is checked
- σ_{bc} : Flexural compressive stress due to bending moment acting around minor axis
- σ_{bao} : Upper limit of allowable flexural compressive stress without consideration of local buckling
- σ_{ea} : Allowable Euler buckling stress around minor axis
- σ_{cag} : Allowable axial compressive stress without consideration of local buckling
- σ_{cal} : Allowable stress for local buckling
- σ_{cao} : Upper limit of allowable axial compressive stress without consideration of local buckling
- ℓ_e : Effective buckling length specified in each division (m)

(Unit: kgf/cm^2)

Here, the load condition was set to be equal to the live loads so as to maximize the main girder axial force at the main tower position, which was determined on the basis of results of the influence line analysis conducted separately. In addition, we obtained buckling eigenvalues using a linearized buckling eigenvalue analysis, under the application of the severest live load described above. In this stability check, the properties of assumed cross section was used.

Table 3 shows results of the stability check. λ in the table represents the minimum buckling eigenvalue which provides the in-plane buckling of the main girder. These results show that even Type-1, in which the stayed part length is the largest and the buckling stability is assumed to be the smallest, satisfies the equation of the stability check. The total length of the stayed parts of the center span in Type-1 was approximately 1,400 m, which does not exceed the critical span length of the cable-stayed bridges.

Table 3 Stability check

	Type-1	Type-2	Type-3
N_G(tf)	40052	24411	13103
$M_{G,in}$(tfm)	13093	11255	10443
$I_{G,in}$(m^4)	22.191	17.373	13.637
A_G(m^2)	2.469	1.913	1.516
ℓ_e(m)	138	125	114
λ	6.012	9.506	16.663
Grade of material	SM570	SM490Y	SM400
(kgf/cm^2)	2600	2100	1400
Stability check	0.93	0.89	0.91

4. Characteristics of coupled flutter

4.1 Natural vibration characteristics

Prior to the coupled flutter analysis, we conducted a natural vibration analysis. As a part of the results of the analysis, *Figure 4* shows diagrams and vibration frequencies of the most dominant basic modes (1st symmetric deflection mode and 1st symmetric torsion mode). The deflection frequency increases with increasing suspended part length, whereas torsional frequency tends to decrease. Judging from the results using these two modes, the frequency ratio increases as the bridge type approaches that of a suspension bridge.

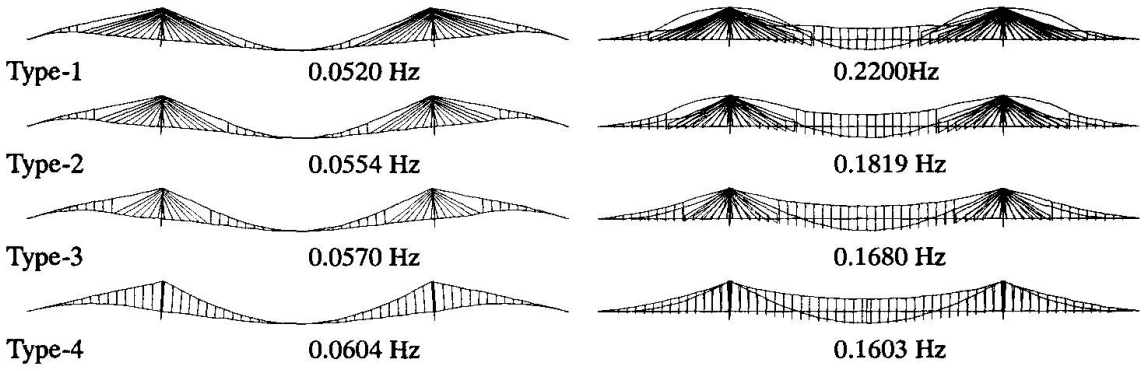

a) 1st symmetric deflection mode b) 1st symmetric torsion mode

Fig. 4 Basic modes by natural vibration analysis

4.2 Estimation of critical wind velocity

We estimated the critical wind velocity of flutter using a coupled flutter analysis based on the modal analysis, by applying the unsteady aerodynamic force based on the plate-wing theory and considering the natural vibration mode up to the 40th mode [5].

Figure 5 shows a relationship between critical wind velocity and weight of steel. The results show that the critical wind velocities were 76, 71, 65 and 63 m/s for cable-stayed suspension bridges Type-1, Type-2, Type-3 and the Type-4 suspension bridge, respectively, indicating that aerodynamic stability of the cable-stayed suspension bridges is superior compared to that of the suspension bridge. The results also show that in cable-stayed suspension bridges, critical wind velocity increases with increasing stayed part length. This is because the increased stayed part length leads to an increase in the rigidity of the entire structure.

For Type-2 and Type-4 bridges, the cross sections of the main girder were changed to twice and then four times of the original value, and the critical wind velocity was calculated. The relationship between the calculated critical wind velocity and total steel weight is also shown in *Figure 5*. If we attempt to ensure the same critical wind velocity for both Type-2 and Type-4, then the Type-4 suspension bridge must have a fairly large value of steel weight. If we attempt to ensure a critical wind velocity of 80 m/s only by an increase in the cross sectional area of the main girder, then the total steel weight of Type-2 cable-stayed suspension bridge should be approximately 300,000 tf, and that of Type-4 suspension bridge should be approximately 360,000 tf as shown in *Figure 5*. Thus, the increase in the total steel weight required for Type-2 is approximately 30% relative to the original weight. In the actual design, the aerodynamic stability of the bridges cannot be ensured using such a simple method; however, in cases of ultra-long span bridges, we can predict that cable-stayed suspension bridges are advantageous over suspension bridges.

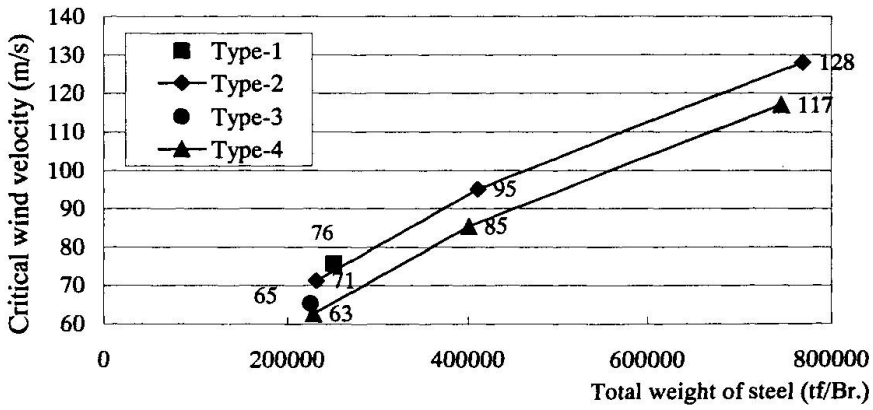

Fig. 5 Relationship between critical wind velocity and weight of steel

5. Applicability of cable-stayed suspension bridges to ultra-long span bridges

The characteristics of the cable-stayed suspension bridges are summarized based on the results of the above investigations, and their applicability to ultra-long span bridges is discussed.

(1) Variety of design and feasibility of the side-span ratio can be improved by appropriately setting lengths of suspended and stayed parts. This implies that different structural systems can be selected in accordance with various conditions such as the side-span ratio and span length, and amount of the axial force and the bending moment of the main girder can be controlled. In addition, since earth-anchored stayed cables are used as the main cables of the side span, characteristics of the earth-anchored cable-stayed bridges can be utilized.

(2) Since a stayed part and a suspended part can be constructed simultaneously in the construction of the main girder, the construction period can be shortened. Furthermore, the main girder of the stayed part can be constructed using a cantilever erection method, following the completion of the main tower.

(3) Regarding the aerodynamic stability, the rigidity of the entire bridge can be increased by setting appropriate stayed part lengths. Thus, superior aerodynamic stability can be obtained as compared to the suspension bridges. In addition, various measures for ensuring the aerodynamic stability can be adopted, taking advantage of the large degree of structural freedom.

(4) In ultra-long span suspension bridges, the weight of the main cables, which account for a large portion of the construction cost, becomes significantly high. Therefore, in most cases, cable-stayed suspension bridges with low cable weight can be economically advantageous over suspension bridges.

Thus, the cable-stayed suspension bridges can be sufficiently competitive, compared to suspension bridges, in terms of ultra-long span bridges, as they make use of the advantages of both the suspension bridge and the cable-stayed bridge, while compensating for their disadvantages at the same time.

6. Conclusions

To investigate the applicability of cable-stayed suspension bridges as ultra-long span bridges, we executed trial designs of three types of the cable-stayed suspension bridges with different suspended part lengths, and confirmed that the cable-stayed suspension bridges can be sufficiently competitive, compared with suspension bridges, in terms of economic efficiency. In the cable-stayed suspension bridges, aerodynamic stability, which significantly influences the feasibility of ultra-long span bridges, can be improved while maintaining economic efficiency comparable to suspension bridges. In terms of buckling stability, which also influences the feasibility of ultra-long span bridges, no problem was found in the safety checking of the cable-stayed suspension bridges; namely, the total length of the stayed parts does not exceed critical span length of the cable-stayed bridge. Furthermore, the construction period can be shortened.

As shown, cable-stayed suspension bridges can be effectively used as ultra-long span bridges with a span length of over 2,000m and can be highly economical and practical as compared to the suspension bridges.

References

[1] K.Nomura, S.Nakazaki, N.Narita, K.Maeda, H.Nakamura: "Structural characteristic and economy of cable supported bridges with long span", Journal of Structural Engineering, Vol.41A, 1995. (in Japanese)
[2] N.Narita, K.Maeda, K.Nomura, S.Nakazaki, H.Nakamura: "Feasibility study on Dischinger-type cable-stayed suspension bridges as a type of ultra-long span bridges", Journal of Constructional Steel, Vol.4, 1996. (in Japanese)
[3] Honshu-Shikoku Authority: Specifications on Superstructure Design, 1989. (in Japanese)
[4] Japan Road Association: Specifications for Highway Bridges, 1996. (in Japanese)
[5] M.Iwamoto: Prediction of aerodynamic behavior of cable supported bridges, Ph.D. thesis, University of Tokyo, 1995. (in Japanese)